1 **SARS-CoV-2 Spike Protein Induces Hemagglutination: Implications for COVID-19**
2 **Morbidities and Therapeutics and for Vaccine Adverse Effects**
3

4 Celine Boschi[1], David E. Scheim[2*], Audrey Bancod[1], Muriel Millitello[1], Marion Le Bideau[1],
5 Philippe Colson[1], Jacques Fantini[3], Bernard La Scola[1*]

6
7 [1] MEPHI, Aix-Marseille Université, Institut de Recherche pour le Développement (IRD),
8   Assistance Publique - Hôpitaux de Marseille (AP-HM), IHU Méditerranée Infection, 13005
9   Marseille, France
10 [2] US Public Health Service, Commissioned Officer, Inactive Reserve, Blacksburg, VA 24060,
11   USA
12 [3] INSERM UMR S 1072, Aix-Marseille Université, 13015 Marseille, France
13

14 ***Correspondence:** dscheim@alum.mit.edu, Tel.: +1 540 3208013; bernard.la-scola@univ-
15 amu.fr, Tel.: +33 413732401

16
20

21 **ABSTRACT**

22 Experimental findings for SARS-CoV-2 related to the glycan biochemistry of coronaviruses

23 indicate that attachments from spike protein to glycoconjugates on the surfaces of red blood cells

24 (RBCs), other blood cells and endothelial cells are key to the infectivity and morbidity of COVID-

25 19. To provide further insight into these glycan attachments and their potential clinical relevance,

26 the classic hemagglutination (HA) assay was applied using spike protein from the Wuhan, Alpha,

27 Delta and Omicron B.1.1.529 lineages of SARS-CoV-2 mixed with human RBCs. The

28 electrostatic potential of the central region of spike protein from these four lineages was studied

29 through molecular modeling simulations. Inhibition of spike protein-induced HA was tested using

30 the macrocyclic lactone ivermectin (IVM), which is indicated to bind strongly to SARS-CoV-2

31 spike protein glycan sites. The results of these experiments were, first, that spike protein from

32 these four lineages of SARS-CoV-2 induced HA. Omicron induced HA at a significantly lower

33 threshold concentration of spike protein than for the three prior lineages and was much more

34 electropositive on its central spike protein region. IVM blocked HA when added to RBCs prior to

35 spike protein and reversed HA when added afterwards. These results validate and extend prior

36 findings on the role of glycan bindings of viral spike protein in COVID-19. They furthermore

37 suggest therapeutic options using competitive glycan-binding agents such as IVM and may help

38 elucidate rare serious adverse effects (AEs) associated with COVID-19 mRNA vaccines which

39 use spike protein as the generated antigen.

INTRODUCTION

Key to the infectivity and morbidity of SARS-CoV-2 are glycans that protrude tangentially from 22 N-linked glycosylation sites on each monomer of its spike protein.[1-5] These N-glycans, several of which are capped with terminal sialic acid (SA) moieties, sweep back and forth across spike protein like windshield wipers, partially shielding it from antibody binding.[1,2,6,7] For SARS-CoV-2 and several other coronaviruses, these N-glycans serve as appendages for the virus to make its initial attachments to glycoconjugates on the host cell surface.[1,8-13] These glycoconjugates confer a negative electrostatic potential on the surfaces of host cells such as red blood cells (RBCs),[14,15] platelets[16] and endothelial cells,[17] additionally facilitating attachments by positively charged SARS-CoV-2 spike protein prior to viral fusion to ACE2 for replication.[8,18-20] For endothelial cells of blood vessel linings, for example, the disparity between 28,000 SA-tipped CD147 receptors and 175 ACE2 receptors per cell[21] provides a supporting indication of the role of glycans in widespread endothelial damage reported in COVID-19 patients.[22,23]

The RBC has an especially dense surface distribution of SA, 35 million SA molecules per cell, arrayed on its sialoglycoprotein coating mainly as terminal residues of glycophorin A (GPA).[14,15] SA in its predominant human form, Neu5Ac, is the most common terminal residue of GPA on human RBCs, with the other terminal monosaccharides of GPA matching those on SARS-CoV-2 spike N-glycans.[2,5] Through attachments to viruses via this GPA surface coating, RBCs and other blood cells can serve a host defense role,[14,24,25] however these RBC clumps can be vascularly obstructive to the host's detriment. Aggregates of RBCs have indeed been found in the blood of most[26,27] or a third[28] of COVID-19 patients in three clinical studies. In a study that examined the blood of hospitalized COVID-19 patients using immunofluorescence analysis, SARS-CoV-2 spike protein punctae were found on 41% of their RBCs.[29] *In vitro*, SARS-CoV-2 spike protein and pseudovirus attached to a nanoparticle array bearing SA derivatives.[30] Microarray detection techniques typically fail to detect these spike protein attachments to either SA[31] or CD147,[32] since they are formed through nanoscale multivalent bindings.[1]

This hemagglutinating property of SARS-CoV-2 has important clinical consequences. First, with trillions of RBCs each circulating through narrow pulmonary capillaries about once per minute, even small, dynamically aggregating and disaggregating RBC clumps (as can form even in the absence of pathogens[33,34]) can impede RBC oxygenation. Peripheral ischemia, endothelial damage and vascular occlusion are indeed frequently observed in serious cases of COVID-19, as

71   reviewed.[1,23] In COVID-19 patients, damaged endothelium of pulmonary capillaries is often

72   observed adjoining relatively intact alveoli,[35,36] while hypoxemia is manifested despite normal

73   breathing mechanics.[22,35,37-39] These morbidities of COVID-19 parallel those of severe malaria, in

74   which clumping of parasite-infected RBCs to other RBCs via SA terminal residues and endothelial

75   cytoadhesion also often result in fatal outcomes.[1]

76   Although the blood cell types and processes entailed in clumping, clotting and vascular

77   obstruction of COVID-19 are wide ranging, virally induced hemagglutination (HA) is a central

78   event that is amenable to *in vitro* study. The classic HA assay was used here to study this, using

79   cell culture supernatants and SARS-CoV-2 trimeric spike protein. Indeed, SARS-CoV-2 spike

80   protein mixed with human whole blood caused RBC aggregation,[40] while spike protein from two

81   other coronavirus strains also induced HA.[41,42] The HA assay can be applied further to study HA

82   inhibitory effects of agents that bind to sites on spike protein, potentially shielding them from

83   attachments to host cells. Several *in silico* studies[1] have found that the macrocyclic lactone

84   ivermectin (IVM) binds with high affinity to subdomains on SARS-CoV-2 spike protein, including

85   several glycosylated binding sites.[43] IVM achieved Nobel prize-honored distinction for success

86   against global parasitic scourges[44] but is of disputed efficacy in the treatment of COVID-19, as

87   indicated, for example, by the disparity in the conclusions of this editorial[45] and its key cited meta-

88   analysis.[46]

89   The goals of this study were to determine whether principles of glycobiology as established

90   for coronaviruses, and in particular for SARS-CoV-2, can be validated using the classic HA assay,

91   to test whether HA inhibition is achieved by an agent indicated to competitively bind to those

92   glycans and to determine the comparative hemagglutinating potencies of the Wuhan virus and its

93   Alpha, Delta and Omicron B.1.1.529 variants. The clinical relevance of testing HA induced by

94   SARS-CoV-2 using spike protein rather than whole virus and the utility of additionally testing for

95   HA inhibition via competitive glycan binding using IVM was suggested in an earlier study.[1] The

96   differences in electrostatic potential of the spike protein of these four variants were studied using

97   molecular modeling and related these to their HA-inducing potencies as experimentally observed.

98   **RESULTS**

99   **Tests for Hemagglutination (HA) and for its inhibition and reversal by IVM**

100   In the HA experiment, for the Wuhan, Alpha and Delta lineages we observed HA at a spike

101   protein concentration of 1.06 ng/µL and above, but not below. For the Omicron spike protein, we

102   observed HA at a minimum concentration of 0.13 ng/µL and above, but not below (Figures 1-2,

103   Table 1).
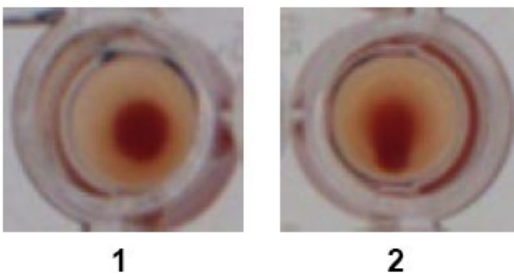
104   **Figure 1**. Sample images of wells in which HA occurred (1; no teardrop visible) and HA did not
105   occur (2; teardrop visible)

106
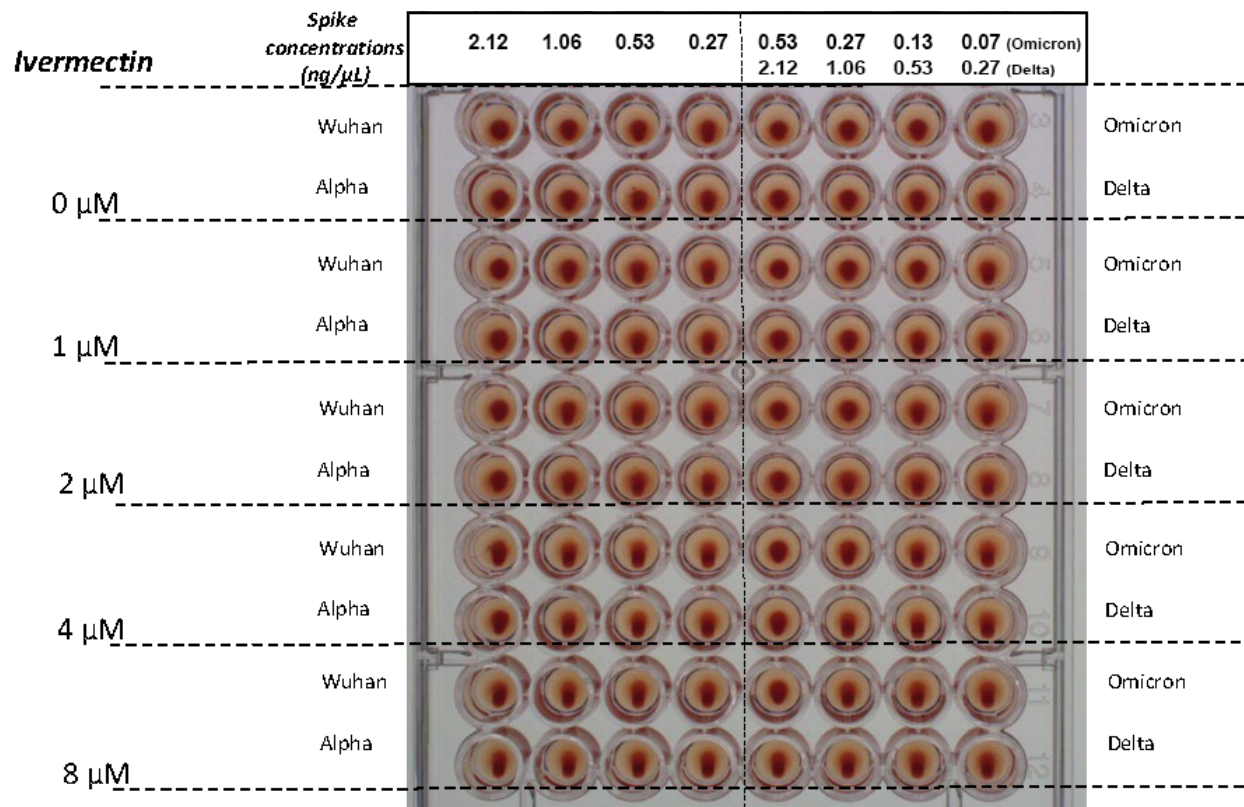
107   **Figure 2.** HA as induced by spike protein concentrations of 0.27, 0.53, 1.06 and 2.12 ng/µL for
108   the Wuhan, Alpha and Delta strains of SARS-CoV-2 and at spike protein concentrations of 0.07,
109   0.13, 0.27 and 0.53 ng/µL for Omicron. Effects on reversal of HA are shown for IVM at
110   concentrations of 1, 2, 4 and 8 µM added 30 min after RBCs and spike protein. Similar results
111   were obtain for inhibition of HA by IVM (not pictured), with differences described in the Results
112   section and summarized in Table 1.

113   In the HA inhibition experiment, IVM added to 2.5% RBC solution to attain a concentration

114   of at 1 µM at 30 minutes prior to spike protein partially inhibited HA, with HA observed at a spike

115   protein concentration of 2.12 ng/µL for the Wuhan, Alpha and Delta and of 0.27 ng/µL for the

116   Omicron viral lineages. With IVM at 2 µM, complete inhibition of HA is observed for the Wuhan,

117   Alpha and Delta lineages. For Omicron, IVM at 4µM is needed to totally block HA.

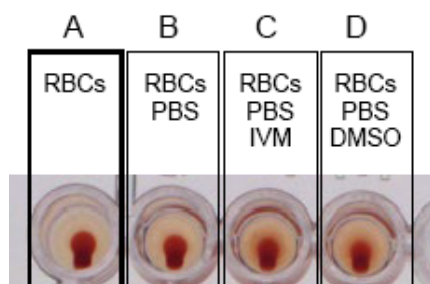118   In the HA reversal experiment, concentrations of IVM needed to reverse HA at the highest

119   concentration of spike tested were 1µM and 2 µM for the Wuhan/Alpha and delta/omicron viral

120   lineages respectively.

121   HA was not observed with cell culture supernatants of any SARS-CoV-2 strain.

122   In the control experiments, RBC alone did not exhibit HA. RBCs mixed with PBS likewise

123   did not exhibit. The addition of IVM to 50 µL of 2.5% RBCs to attain a concentration of at 8 µM

124   did not cause hemolysis or induce HA. A solution of 2.5% DMSO and 97.5% water, the solvent

125   for IVM, did not block or reverse HA (Figure 2 and 3).

126

127   **Table 1**. Minimum concentrations of recombinant spike protein (ng/µL) needed to induce HA
128   when added to RBC solution, and concentrations of IVM (µM) needed to inhibit or reverse this
129   induced HA. Tests to determine these values were each done in triplicate.
130

| Variant	Minimum spike protein concentration to induce HA (ng/µL)	Highest spike protein concentration tested for HA (ng/µL)	Minimum IVM concentration to inhibit HA at highest spike concentration (µM)	Minimum IVM concentration to release HA (µM) at highest spike concentration
Wuhan	1.06	2.12	1	1
Alpha	1.06	2.12	1	1
Delta	1.06	2.12	1	2
Omicron	0.13	0.53	1	2

131

132

Figure 3. Controls: (A) RBCs alone, (B) RBCs with PBS, (C) RBCs with PBS and IVM and (D) RBCs with PBS and DMSO. No HA is observed.

Western blot and quantification analysis

135

136   The results for quantification analysis by Western blot of spike protein in cell culture

137   supernatants are presented in Figure 4. This shows that its spike concentration is below the

138   concentration thresholds for induction of agglutination. Indeed for the supernatant of the Wuhan

139   strain in cell culture at 48 h post viral infection, the concentration of N-glycosylated spike protein

140   is approximately 0.7 ng/µL, which dilutes to half that concentration when added to wells,

141   approximately three times lower than the minimum concentration 1.06 ng/µL of recombinant spike

142   found to induce HA in the HA experiment described above.

143
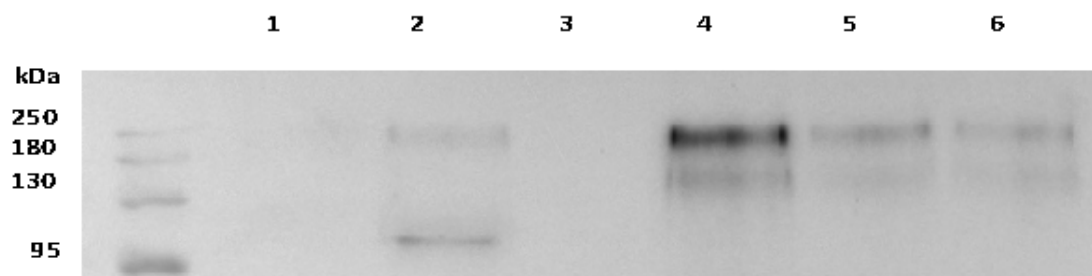
144   **Figure 4.** Quantification by Western blot analysis of spike protein in cell culture supernatants.
145   Lines 1 and 2: cell culture supernatants infected with SARS-CoV-2, Wuhan strain, harvested at 24
146   and 48h respectively. Line 3: non-infected cell culture supernatant. Lines 4, 5 and 6: recombinant
147   SARS-CoV-2 spike protein at 2.25, 1.25 and 0.56 ng/µL respectively.

Molecular modeling

148

149   Since the surface of RBCs is electronegative due to a high expression of anionic sialic acids

150   in membrane proteins and gangliosides, we used molecular modeling simulations to study the

151   electrostatic surface potential of the spike proteins used in the present study. We focused our

152   attention on the central area of the spike trimers which is formed by the receptor binding domain

153   (RBD) of each monomer. The electrostatic potential of the central area of the spike trimers

154   increased exponentially from the Wuhan initial lineage to the Omicron variant (Figure 5, lower

155   panel). This was caused by a progressive decrease in electronegative zones (colored in red) and a

156   concomitant increase in electropositivity (blue zones). The increase was modest between Wuhan

157   and Alpha, larger for Delta, and reached very high levels for Omicron. As depicted in the upper

158   panel of Figure 5, these variations in net positive electric charge between the four SARS-CoV-2

159   strains considered here have implications for induction of HA, since electropositivity mitigates the

160   electrostatic repulsion between negatively charged RBC surfaces.
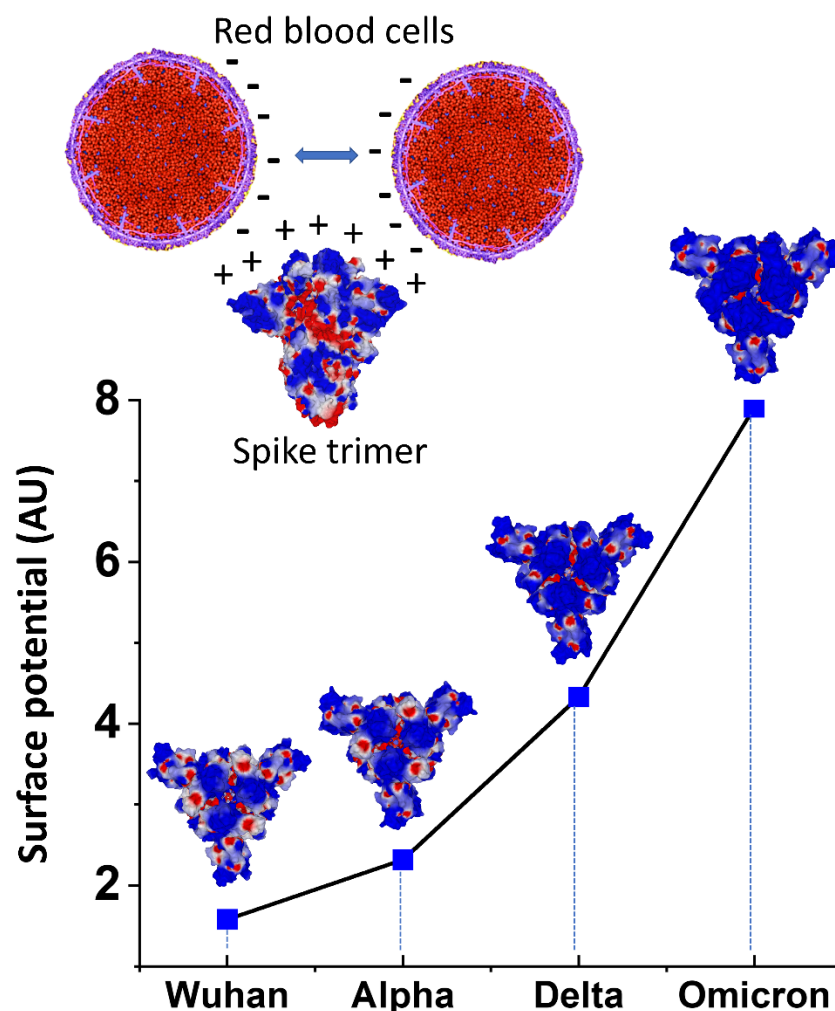
Figure 5. **Electrostatic surface potential of SARS-CoV-2 spike trimers**. **Upper panel.** Under physiological conditions, RBCs maintain separation from each other due to a repulsive electric zeta potential between their negatively charged surfaces. The electropositive surface of spike protein neutralizes this zeta potential, allowing closer contacts between RBCs. **Lower panel.** For all variants, the electrostatic surface potential of the spike trimer is more electropositive in the central area formed by the RBD of each monomer. Quantitative analysis of the surface potential (in AU=arbitrary units) shows an exponential increase from the Wuhan to Omicron lineages.

DISCUSSION

For all four SARS-CoV-2 lineages tested, Wuhan, Alpha, Delta and Omicron BA.1, spike protein mixed with human RBCs induced HA. This result provides an *in vitro* counterpart to the RBC clumping found, for example, in the blood of most[26,27] or a third[28] of COVID-19 patients in three clinical studies, and reinforces indications that such blood cell aggregation is key to the

174   morbidities of this disease. HA-associated vascular obstruction in COVID-19 was further

175   demonstrated in Zebrafish embryos, which have capillary diameters[47] and blood cell glycosylation

176   patterns[48] similar to those of humans. SARS-CoV-2 spike protein injected into a Zebrafish embryo

177   vein caused the formation of small RBC clumps and an associated reduction in blood flow velocity

178   within 3-5 minutes after injection.[49] Also, in various *in vivo* or *in vitro* studies, SARS-CoV-2 spike

179   protein S1 was found to cause endothelial, pulmonary and neuronal damage as well as platelet-

180   thrombi formation and microclots.[40,50-52]

181   In addition to the glycan bindings reviewed above, electrostatic attraction could promote

182   attachments between RBCs and SARS-CoV-2 spike protein underlying the observed HA. As

183   indicated here by molecular modeling simulations, the SARS-CoV-2 spike protein central region

184   has a net positive charge, which yields an attractive force to the negatively charged RBC surface

185   and also mitigates the repulsive electrostatic force between RBCs. This result is consistent with

186   prior determinations of a net positive electrostatic potential of SARS-CoV-2 spike protein.[19,53]

187   Regardless of whether glycan bindings or electrostatic attraction is the predominant underlying

188   force, the HA observed here suggests, more generally, that spike protein attachments to other cells

189   such as platelets and endothelial cells may be implicated in COVID-19 morbidities, these two

190   cells, like RBCs, having dense surface distributions of SA-tipped glycans[1] and corresponding

191   negative surface charges.[16,17] These attachments can manifest clinically in damage to endothelial

192   cell induced by virions or free spike proteins, marked by traces of spike protein,[23,35,51] and in the

193   formation of fibrin-hardened clots that incorporate platelets, neutrophils and other blood cells,[54]

194   potentially seeded by RBC clumps.

195   The much stronger HA-inducing effect of spike protein of the SARS-CoV-2 Omicron variant

196   vs. the prior lineages tested here, with thresholds of concentration for HA induction of 0.13 ng/μL

197   for Omicron vs. 1.06 ng/μL for the Wuhan, Alpha and Delta lineages, was an intriguing result.

198   Under the hypothesis that RBC clumping underlies the morbidities of COVID-19, especially those

199   related to diminished efficiency of RBC oxygenation, this finding appears paradoxical, since

200   percentages of patients having respiratory distress or requirements for oxygen or mechanical

201   ventilation were all sharply less for Omicron as compared with prior viral lineages.[55] Yet as noted

202   above, increased binding affinities of viral spike protein for host cell glycoconjugates beyond

203   optimal levels are counterproductive for infectivity, as this results in increased snagging of newly

204   replicated virions on sialoside-binding sites of host cells and viral snagging on SA-rich non-

205   infectious targets.[1,23,56] The increased glycan-binding propensity of Omicron vs. prior lineages, as

206   indicated by its increased HA-inducing activity, may thus limit the ability of an Omicron virion

207   from an infected alveolar cell to penetrate the juncture between alveolar and capillary basal

208   surfaces and infect an endothelial cell or otherwise enter the blood stream.

209   Likewise, increased net positive charge of the spike protein of Omicron vs. prior lineages

210   could also increase viral snagging and limit penetration into the blood stream. Further confounding

211   factors are indications from molecular modeling that while the overall electrostatic potential of

212   Omicron spike protein is more positive than for prior lineages, its N-terminal domain (NTD) is

213   less positive than for prior lineages,[53,57,58] and its sialic acid binding affinity is greater.[59] It has also

214   been proposed, again based upon *in silico* analysis, that decreased binding affinity of mutated

215   residues on the Omicron spike protein to a cellular receptor implicated in thromboembolic and

216   neurological complications of COVID-19, α7nAChR, could also account for decreased morbidity

217   of this viral variant.[60]

218   IVM, an electrically neutral molecule,[61] has been found *in silico* to attach with strong affinity

219   to 10 glycan binding sites on the spike protein of the Alpha through Delta variants,[43] which

220   suggests that competitive inhibition of spike protein attachments to host cell glycoconjugates could

221   be its means of HA inhibition. IVM at concentrations of 1-2 µM for the four different viral lineages

222   inhibited HA when added concurrently with spike protein and also reversed HA that had been

223   induced by the prior addition of spike protein. This HA-reversal effect could account for sharp

224   increases observed within 24 hours after administration of IVM of pre-treatment depressed SpO2

225   levels in severe COVID-19 patients, as summarized in Figure 6 from the most recent of three

226   clinical studies reporting this effect.[62] The inhibition of HA by IVM as reported here parallels the

227   prevention of RBC clumping in Zebrafish embryos by heparan sulfate, a glycosaminoglycan

228   likewise indicated to strongly bind to SARS-CoV-2 spike protein,[49,63] when coinjected with spike

229   protein.[49] It is noteworthy that the scattered RBC clumps observed in this Zebrafish embryo study,

230   as with those observed in the blood of COVID-19 patients,[26-28] are much smaller than the

231   macroscopic-scale HA—clusters of extensively interlaced RBCs—observed in this study. It is

232   therefore likely that smaller concentrations of spike protein and IVM would be required to,

233   respectively, induce and reverse RBC clumps of clinical relevance. Thus, the peak plasma level of

234   IVM of approximately 412 nM as attained about four hours after a standard oral dose of 200-350

235   µg/kg[1] appears to be in a range that could achieve clinical effects analogous to HA reversal observed in this

236   study at IVM concentrations of 1-2 µM.

237   The HA-inducing activity of SARS-CoV-2 spike protein, which is especially potent for

238   Omicron, raises questions as to potential risks for COVID-19 mRNA vaccines, which use spike

239   protein as the generated antigen, even though serious adverse effects (AEs) linked to spike protein,

240   such as myocarditis,[64-66] are rare. Detectable levels of SARS-CoV-2 spike protein and S1 in serum

241   or plasma have been found to persist as long as 50 days following such vaccinations.[67-69] The

242   possibility that spike protein migrating into the blood stream could in rare cases prompt such HA-

243   associated AEs is suggested, for example, by a study of 1,006 subjects experiencing AEs after

244   receiving a Pfizer/BioNTech or Moderna mRNA vaccination which found a significant degree of

245   RBC aggregation in the blood of 948 of those subjects.[70] These risks may be increased for younger

246   age groups, with 301 adolescents of 13-18 years of age who received two doses of the BNT162b2

247   mRNA COVID-19 vaccine in one study having a 29.2% rate of cardiac AEs, ranging from

248   tachycardia or palpitation to myopericarditis.[71] The investigators considered chest pain, which

249   occurred at a 4% incidence, "an alarming side effect," however myopericarditis cases were mostly

250   mild and temporary.

251   Additional experiments of interest in follow-up to this study include microscopic detection to

252   check for initial formation of RBC clumping at spike protein concentrations lower than those

253   which induce HA. Also, the Zebrafish study as described as above could be replicated using IVM

254   instead of heparan sulfate as the blocking agent. Finally, HA could be tested as in this experiment

255   but using RBCs supplemented with human serum albumin (HSA) at a physiological concentration.

256   If IVM were to bind to spike protein glycans at the same molecular region as that which binds to

257   HSA, that could significantly limit its HA-inhibitory effect, since 93% of IVM binds to serum

258   proteins, mainly HSA, in blood,[72] and that 93% of IVM would then be rendered inactive for this

259   effect. If, on the other hand, IVM were to bind to spike protein glycans and to HSA each at different

260   regions, then HSA, a large molecule (molecular mass of 66.5 kDa, vs. 875.1 for IVM), could

261   considerably boost the HA-inhibitory effect of IVM through steric interference.

262   **MATERIALS AND METHODS**

263   **Source and preparation of red blood cells**

264   Red blood cells (RBCs) were provided by the "Establishment Français du Sang" (EFS) from

265   blood bag donors qualified as "non-therapeutic blood bag" (Convention N°7828). Twenty ml of

266   whole blood (with anticoagulant EDTA) were added to a 50 ml conical tube and filled with 30 ml

267   of PBS at pH=7.2 before centrifugation at 800 xg for 10 min. Then, the supernatant was discarded

268   and replaced by fresh PBS. This procedure was repeated again twice. After the last centrifugation,

269   RBCs were diluted in PBS at a final concentration of 2.5%. RBCs were then stocked one week at

270   4 °C.

271   **Spike proteins preparation**

272   Recombinant spike proteins (BioServUK Sheffield, United Kingdom) of these four following

273   SARS-CoV-2 strains were used for this experiment: Wuhan, Alpha, Delta and Omicron BA.1

274   (BSV-COV-PR-33, BSV-COV-PR-65, BSV-COV-PR-97 and BSV-COV-OM-0.1, respectively).

275   Four concentrations of spike protein were prepared for each of these viruses by diluting stock

276   suspension in phosphate-buffered saline (PBS). Spike protein of each viral strain was dissolved in

277   PBS and added to wells at final increasing concentrations of 0.27 ng/µL, 0.53 ng/µL, 1.06 ng/µL

278   and 2.12 ng/µL for the Wuhan, Alpha and Delta lineages and of 0.07 ng/µL, 0.13 ng/µL, 0.27

279   ng/µL and 0.53 ng/µL for the Omicron variant.

280   **Cells and SARS-CoV-2 strains preparation**

281   Vero E6 cells (ATCC-CRL-1586) were cultured as in previously described conditions[73-75] in

282   medium (MEM, Gibco, USA) with 2 mM L-glutamine and 10% fetal bovine serum (FBS) at 37

283   °C in a 5% CO2 incubator. We infected Vero E6 with four viral strains genotyped by whole

284   genome next-generation sequencing (NGS) as belonging to: Pangolin lineage B.1.1[76] (the first

285   major lineage following the Wuhan genotype that circulated during the first epidemic period in

286   France, hereinafter designated "Wuhan") and three variants: Alpha (B.1.1.7), Delta (B.1.617.2)

287   and Omicron BA.1 (B.1.1.529). Culture supernatants were harvested 24 h post-viral infection and

288   then passed through 0.22 µM pore-sized filters (Merck Millipore, Carrigtwohill, Ireland) to

289   remove cell and debris and obtain viral suspension for experiments.

290   **Western blot and quantification analysis**

291   Supernatants from Wuhan SARS CoV-2 infected cells prepared as described above or

292   uninfected cells and commercial spike were lysed with 2x Laemmli Sample Buffer (#1610737,

293   Bio-Rad, Hercules, CA, USA) with DTT (#EU0006-B, Euromedex, France) added as reducing

294   agent and then heated at 95 °C for 5 min. Proteins were separated by 10% SDS-polyacrylamide

295   gel electrophoresis (Laemmli, 1970) and Western-blotted on a nitrocellulose membrane. After one

296   h of saturation in 5% nonfat dry milk with 0.3% Tween-20 in PBS, the membrane was incubated

297 overnight with SARS/SARS-CoV-2 Coronavirus Spike Protein (subunit 1) rabbit polyclonal
298 antibody (Thermo Fisher scientific, France) at a dilution of 1:1000 in the same buffer as for
299 saturation. After this first incubation, the membrane was washed 10 min three times in PBS 1X-
300 Tween buffer and then incubated for one h at room temperature with peroxydase labeled anti-
301 rabbit donkey antibody (#NIF 824 ECL Rabbit IgG, HRP-linked whole Ab, Sigma-Aldrich Life
302 Science, USA) diluted in saturation buffer at 1:1000. After this second incubation, the membrane
303 was rinsed 10 min three times in PBS 1X-Tween buffer before ECL (Western Blotting Substrate,
304 # W1001 Promega, Madison, WI, USA) revelation by image acquisition with the Fusion Fx
305 chemiluminescence imaging system (Vilber Lourmat, Marne-la Vallée, France). Quantification in
306 each well was calculated by measuring band intensities using ImageQuant analysis software (GE
307 Healthcare Europe). Protein markers (New England Biolabs, #P7719S) were used for molecular
308 mass determination.

309 **IVM preparation**

310 IVM was supplied by Sigma Aldrich (St Quentin Fallavier, France). Stock solution was
311 diluted in 2.5% of DMSO and 97.5% of water. IVM, 20 µL in volume, was added in designated
312 wells to reach final concentrations of 1, 2, 4 and 8 µM, as specified.

313 **Tests for Hemagglutination (HA) and for its inhibition and reversal by IVM**

314 Three sets of experiments were performed to test for HA induced by SARS-CoV-2 spike
315 protein and then for HA inhibition and reversal by IVM. To test for HA, using a 96 micro-well
316 plate, 50 µL of 2.5% RBCs in PBS was added to wells together with 62 µL of diluted spike proteins
317 at specified concentrations. An additional 20 µL of PBS was added to attain the same total fluid
318 volume as used in IVM inhibition and reversal experiments. This mixture was let sit for 30 min at
319 room temperature under gentle agitation. Then, the plate was tilted for at least 30 seconds, after
320 which, if HA had not occurred a teardrop could be observed at the bottom of the well consisting
321 of settled RBCs (Figure 1). This teardrop was not observed if HA had occurred, i.e., if a network
322 of linked, agglutinated RBCs had formed, as described previously.[77] To test for inhibition of HA
323 by IVM, 50 µL of RBCs were mixed with 20 µL of IVM at specified concentrations ranging from
324 1-8 µM and let sit for 30 min at room temperature under gentle agitation. Then 62 µL of spike
325 protein was added at specified concentrations, wells were let sit for an additional 30 min at room
326 temperature under gentle agitation, and HA was determined as in above. Finally, to test for reversal
327 of HA by IVM, 50µL of RBCs were mixed with 62 µL of spike proteins for 30 min to determine

328   HA as above. Then 20 µL of IVM were added at specified concentrations, wells were let sit for

329   additional 30 min at room temperature under gentle agitation and then the plate was tilted at least

330   30 seconds and wells were rechecked for HA as described in above.

331   The following control experiments were performed. Fifty µl of RBCs deposited alone in the

332   wells allows to check their absence of agglutination. Twenty µL of PBS were added to 50 µL of

333   RBCs to verify absence of HA. The potential for induction of HA by IVM was tested by adding it

334   at the highest concentration used (8 µM) to 50 µL of 2.5% RBCs. In order to test whether DMSO

335   blocked or reversed HA, we also performed the HA inhibition and reversal experiments described

336   respectively above using the solvent for IVM, 2.5% DMSO and 97.5% water, but without IVM.

337   The HA experiment was then done with viral suspensions for each viral strains by adding to

338   the wells the same volume of viral supernatant as for commercial spike suspensions.

339   Each experiment was done in triplicate.

340   **Molecular modeling simulations**

341   A complete structure of the reference spike protein was generated from the original 20B strain

342   (pdb: 7bnm) as previously described.[78] All gaps in the pdb file were fixed by inserting the missing

343   amino acids with the protein structure prediction service Robetta [https://robetta.bakerlab.org/].[53,79]

344   This source file model was used to introduce the specific mutational profiles of the indicated

345   Alpha, Delta and Omicron variants with the MUTATE tool of Swiss-PdbViewer.[53,80] Trimeric

346   structures in the closed pre-fusion conformation were constructed with Swiss-PdbViewer by

347   homology with a reference model (pdb: 6VSB). All structures were then submitted to several

348   rounds of energy minimization with the Polak-Robière algorithm.[74] The electrostatic surface

349   potential of the spike trimers was analyzed with Molegro and quantified with ImageJ software as

350   described previously.[78]

351   **CONCLUSIONS**

352   Spike protein from four lineages of SARS-CoV-2 induced HA in human RBCs, which

353   supports other indications that spike protein-induced RBC clumping, as well as viral attachments

354   to other blood cells and endothelial cells, may be key to the morbidities of COVID-19. IVM, a

355   macrocyclic lactone indicated to bind strongly to multiple glycan sites on SARS-CoV-2 spike

356   protein, blocked HA when added to RBCs prior to spike protein and reversed HA when added

357   afterwards, which suggests therapeutic options for COVID-19 treatment using this drug or other

358 competitive glycan-binding agents. The Omicron B.1.1.529 variant had significantly greater HA-
359 inducing activity than the three prior lineages tested, which may relate in part to the finding from
360 molecular modeling that the electrostatic charge of the central region of its spike protein was
361 considerably more positive than for those of the prior lineages. The incongruity between
362 Omicron's increased HA-inducing activity and decreased morbidity may derive from limitations
363 on virion mobility through body tissues associated with increased strength of its glycan binding or
364 electrostatic attraction to host cell surfaces. It is not clear, however, whether this heightened HA-
365 inducing activity of the Omicron variant might potentially increase or decrease the rate of rare HA-
366 associated AEs for Omicron boosters vs. this rate for legacy mRNA COVID vaccines.

367 **Author Contributions:** Conceptualization, DES, JF and BLS; methodology, JF and BLS;
368 validation, CB, PV, JF, BLS; formal analysis, CB, BLS; investigation, AB, MM, MLB; writing—
369 original draft preparation, DES, CB, JF, BLS; writing—review and editing, PC; supervision, JF,
370 BLS; project administration, BLS. All authors have read and agreed to the published version of
371 the manuscript.

375 **Institutional Review Board Statement:** Not applicable.

376 **Informed Consent Statement:** Not applicable.

377 **Conflicts of Interest:** The authors declare no conflict of interest.

378 **Abbreviations:**
379 The following abbreviations are used in this manuscript:

ACE2	angiotensin converting enzyme 2
CD147	cluster of differentiation 147 protein, encoded by the BSG gene
COVID-19	coronavirus disease 2019
GPA	glycophorin A
NTD	N-terminal domain
RBC	red blood cell
RBD	receptor binding domain
RCT	randomized clinical trial
SA	sialic acid
SARS-CoV-2	severe acute respiratory syndrome coronavirus 2

380

381 **References**
382 1. Scheim, D.E. A Deadly Embrace: Hemagglutination Mediated by SARS-CoV-2 Spike Protein at its 22 N-
383 Glycosylation Sites, Red Blood Cell Surface Sialoglycoproteins, and Antibody. *Int. J. Mol. Sci.* **2022**, *23*, 2558.
384 2. Chen, W.; Hui, Z.; Ren, X.; Luo, Y.; Shu, J.; Yu, H.; Li, Z. The N-glycosylation sites and Glycan-binding ability
385 of S-protein in SARS-CoV-2 Coronavirus. *bioRxiv* **2020**, doi:10.1101/2020.12.01.406025.

3. Guo, W.; Lakshminarayanan, H.; Rodriguez-Palacios, A.; Salata, R.A.; Xu, K.; Draz, M.S. Glycan Nanostructures of Human Coronaviruses. *Int J Nanomedicine* **2021**, *16*, 4813-4830.

4. Shajahan, A.; Supekar, N.T.; Gleinich, A.S.; Azadi, P. Deducing the N- and O-glycosylation profile of the spike protein of novel coronavirus SARS-CoV-2. *Glycobiology* **2020**, *30*, 981-988.

5. Gao, C.; Zeng, J.; Jia, N.; Stavenhagen, K.; Matsumoto, Y.; Zhang, H.; Li, J.; Hume, A.J.; Mühlberger, E.; van Die, I.; et al. SARS-CoV-2 Spike Protein Interacts with Multiple Innate Immune Receptors. *bioRxiv* **2020**, doi:10.1101/2020.07.29.227462.

6. Sikora, M.; von Bülow, S.; Blanc, F.E.C.; Gecht, M.; Covino, R.; Hummer, G. Computational epitope map of SARS-CoV-2 spike protein. *PLOS Computational Biology* **2021**, *17*, e1008790.

7. Choi, Y.K.; Cao, Y.; Frank, M.; Woo, H.; Park, S.-J.; Yeom, M.S.; Croll, T.I.; Seok, C.; Im, W. Structure, Dynamics, Receptor Binding, and Antibody Binding of the Fully Glycosylated Full-Length SARS-CoV-2 Spike Protein in a Viral Membrane. *Journal of Chemical Theory and Computation* **2021**, *17*, 2479-2487.

8. Koehler, M.; Delguste, M.; Sieben, C.; Gillet, L.; Alsteens, D. Initial Step of Virus Entry: Virion Binding to Cell-Surface Glycans. *Annual Review of Virology* **2020**, *7*, 143-165.

9. Fantini, J.; Di Scala, C.; Chahinian, H.; Yahi, N. Structural and molecular modelling studies reveal a new mechanism of action of chloroquine and hydroxychloroquine against SARS-CoV-2 infection. *International Journal of Antimicrobial Agents* **2020**, *55*, 105960.

10. Ströh, L.J.; Stehle, T. Glycan Engagement by Viruses: Receptor Switches and Specificity. *Annual Review of Virology* **2014**, *1*, 285-306.

11. Morniroli, D.; Giannì, M.L.; Consales, A.; Pietrasanta, C.; Mosca, F. Human Sialome and Coronavirus Disease-2019 (COVID-19) Pandemic: An Understated Correlation? *Frontiers in Immunology* **2020**, *11*, 1480.

12. Neu, U.; Bauer, J.; Stehle, T. Viruses and sialic acids: rules of engagement. *Curr Opin Struct Biol* **2011**, *21*, 610-618.

13. Nguyen, L.; McCord, K.A.; Bui, D.T.; Bouwman, K.M.; Kitova, E.N.; Elaish, M.; Kumawat, D.; Daskhan, G.C.; Tomris, I.; Han, L.; et al. Sialic acid-containing glycolipids mediate binding and viral entry of SARS-CoV-2. *Nature Chemical Biology* **2022**, *18*, 81-90.

14. Baum, J.; Ward, R.H.; Conway, D.J. Natural selection on the erythrocyte surface. *Mol Biol Evol* **2002**, *19*, 223-229.

15. Aoki, T. A Comprehensive Review of Our Current Understanding of Red Blood Cell (RBC) Glycoproteins. *Membranes (Basel)* **2017**, *7*.

16. Seaman, G.V.F. Electrochemical features of platelet interactions. *Thrombosis Research* **1976**, *8*, 235-246.

17. Strilić, B.; Eglinger, J.; Krieg, M.; Zeeb, M.; Axnick, J.; Babál, P.; Müller, D.J.; Lammert, E. Electrostatic Cell-Surface Repulsion Initiates Lumen Formation in Developing Blood Vessels. *Current Biology* **2010**, *20*, 2003-2009.

18. Boulant, S.; Stanifer, M.; Lozach, P.-Y. Dynamics of virus-receptor interactions in virus binding, signaling, and endocytosis. *Viruses* **2015**, *7*, 2794-2815.

19. Hassanzadeh, K.; Perez Pena, H.; Dragotto, J.; Buccarello, L.; Iorio, F.; Pieraccini, S.; Sancini, G.; Feligioni, M. Considerations around the SARS-CoV-2 Spike Protein with Particular Attention to COVID-19 Brain Infection and Neurological Symptoms. *ACS Chem Neurosci* **2020**, *11*, 2361-2369.

20. Pawłowski, P.H. Additional Positive Electric Residues in the Crucial Spike Glycoprotein S Regions of the New SARS-CoV-2 Variants. *Infect Drug Resist* **2021**, *14*, 5099-5105.

21. Ahmetaj-Shala, B.; Vaja, R.; Atanur, S.S.; George, P.M.; Kirkby, N.S.; Mitchell, J.A. Cardiorenal Tissues Express SARS-CoV-2 Entry Genes and Basigin (BSG/CD147) Increases With Age in Endothelial Cells. *JACC: Basic to Translational Science* **2020**, *5*, 1111-1123.

22. Huertas, A.; Montani, D.; Savale, L.; Pichon, J.; Tu, L.; Parent, F.; Guignabert, C.; Humbert, M. Endothelial cell dysfunction: a major player in SARS-CoV-2 infection (COVID-19)? *Eur Respir J* **2020**, *56*.

23. Scheim, D.E. From cold to killer: How SARS-CoV-2 evolved without hemagglutinin esterase to agglutinate, then clot blood cells in pulmonary and systemic microvasculature. Available online: https://osf.io/sgdj2 (accessed on October 17, 2022).

24. De Back, D.Z.; Kostova, E.; Klei, T.; Beuger, B.; van Zwieten, R.; Kuijpers, T.; Juffermans, N.; van den Berg, T.; Korte, D.; van Kraaij, M.; et al. RBC Adhesive Capacity Is Essential for Efficient 'Immune Adherence Clearance' and Provide a Generic Target to Deplete Pathogens from Septic Patients. *Blood* **2016**, *128*, 1031.

25. Varki, A.; Gagneux, P. Multifarious roles of sialic acids in immunity. *Ann N Y Acad Sci* **2012**, *1253*, 16-36.

26. Berzuini, A.; Bianco, C.; Migliorini, A.C.; Maggioni, M.; Valenti, L.; Prati, D. Red blood cell morphology in patients with COVID-19-related anaemia. *Blood Transfus* **2021**, *19*, 34-36.

27. Melkumyants, A.; Buryachkovskaya, L.; Lomakin, N.; Antonova, O.; Serebruany, V. Mild COVID-19 and Impaired Blood Cell–Endothelial Crosstalk: Considering Long-Term Use of Antithrombotics? *Thromb Haemost* **2022**, *122*, 123-130.

28. Lakhdari, N.; Tabet, B.; Boudraham, L.; Laoussati, M.; Aissanou, S.; Beddou, L.; Bensalem, S.; Bellik, Y.; Bournine, L.; Fatmi, S.; et al. Red blood cells injuries and hypersegmented neutrophils in COVID-19 peripheral blood film. *medRxiv* **2020**, doi:10.1101/2020.07.24.20160101.

29. Lam, L.M.; Murphy, S.J.; Kuri-Cervantes, L.; Weisman, A.R.; Ittner, C.A.G.; Reilly, J.P.; Pampena, M.B.; Betts, M.R.; Wherry, E.J.; Song, W.-C.; et al. Erythrocytes Reveal Complement Activation in Patients with COVID-19. *medRxiv* **2020**, doi:10.1101/2020.05.20.20104398.

30. Baker, A.N.; Richards, S.-J.; Guy, C.S.; Congdon, T.R.; Hasan, M.; Zwetsloot, A.J.; Gallo, A.; Lewandowski, J.R.; Stansfeld, P.J.; Straube, A.; et al. The SARS-COV-2 Spike Protein Binds Sialic Acids and Enables Rapid Detection in a Lateral Flow Point of Care Diagnostic Device. *ACS Central Science* **2020**, *6*, 2046-2052.

31. Hao, W.; Ma, B.; Li, Z.; Wang, X.; Gao, X.; Li, Y.; Qin, B.; Shang, S.; Cui, S.; Tan, Z. Binding of the SARS-CoV-2 spike protein to glycans. *Sci Bull (Beijing)* **2021**, *66*, 1205-1214.

32. Shilts, J.; Wright, G.J. No evidence for basigin/CD147 as a direct SARS-CoV-2 spike binding receptor. *bioRxiv* **2020**, doi:10.1101/2020.07.25.221036.

33. Maeda, N.; Seike, M.; Kon, K.; Shiga, T. Erythrocyte Aggregation as a Determinant of Blood Flow: Effect of pH, Temperature and Osmotic Pressure. In *Oxygen Transport to Tissue X*, Mochizuki, M., Honig, C.R., Koyama, T., Goldstick, T.K., Bruley, D.F., Eds.; Springer US: New York, NY, 1988; 10.1007/978-1-4615-9510-6_68pp. 563-570.

34. Barshtein, G.; Wajnblum, D.; Yedgar, S. Kinetics of linear rouleaux formation studied by visual monitoring of red cell dynamic organization. *Biophys J* **2000**, *78*, 2470-2474.

35. Magro, C.; Mulvey, J.J.; Berlin, D.; Nuovo, G.; Salvatore, S.; Harp, J.; Baxter-Stoltzfus, A.; Laurence, J. Complement associated microvascular injury and thrombosis in the pathogenesis of severe COVID-19 infection: A report of five cases. *Transl Res* **2020**, *220*, 1-13.

36. Menter, T.; Haslbauer, J.D.; Nienhold, R.; Savic, S.; Hopfer, H.; Deigendesch, N.; Frank, S.; Turek, D.; Willi, N.; Pargger, H.; et al. Postmortem examination of COVID-19 patients reveals diffuse alveolar damage with severe capillary congestion and variegated findings in lungs and other organs suggesting vascular dysfunction. *Histopathology* **2020**, *77*, 198– 209.

37. Becker, R.C. COVID-19 update: Covid-19-associated coagulopathy. *J Thromb Thrombolysis* **2020**, *50*, 54-67.

38. Gattinoni, L.; Coppola, S.; Cressoni, M.; Busana, M.; Rossi, S.; Chiumello, D. COVID-19 Does Not Lead to a "Typical" Acute Respiratory Distress Syndrome. *Am J Respir Crit Care Med* **2020**, *201*, 1299-1300.

39. Marini, J.J.; Gattinoni, L. Management of COVID-19 Respiratory Distress. *JAMA* **2020**, *323*, 2329-2330.

40. Grobbelaar, Lize M.; Venter, C.; Vlok, M.; Ngoepe, M.; Laubscher, Gert J.; Lourens, Petrus J.; Steenkamp, J.; Kell, Douglas B.; Pretorius, E. SARS-CoV-2 spike protein S1 induces fibrin(ogen) resistant to fibrinolysis: implications for microclot formation in COVID-19. *Bioscience Reports* **2021**, *41*.

41. Schultze, B.; Gross, H.J.; Brossmer, R.; Herrler, G. The S protein of bovine coronavirus is a hemagglutinin recognizing 9-O-acetylated sialic acid as a receptor determinant. *J Virol* **1991**, *65*, 6232-6237.

42. Callebaut, P.E.; Pensaert, M.B. Characterization and isolation of structural polypeptides in haemagglutinating encephalomyelitis virus. *J Gen Virol* **1980**, *48*, 193-204.

43. Aminpour, M.; Cannariato, M.; Safaeeardebili, M.E.; Preto, J.; Moracchiato, A.; Doria, D.; Donato, F.; Zizzi, E.A.; Deriu, M.A.; Scheim, D.E.; et al. In Silico Analysis of the Multi-Targeted Mode of Action of Ivermectin and Related Compounds. *Computation* **2022**, *10*, 51.

44. Santin, A.D.; Scheim, D.E.; McCullough, P.A.; Yagisawa, M.; Borody, T.J. Ivermectin: a multifaceted drug of Nobel prize-honored distinction with indicated efficacy against a new global scourge, COVID-19. *New Microbes and New Infections* **2021**, *43*, 100924.

45. Abdool Karim, S.S.; Devnarain, N. Time to Stop Using Ineffective Covid-19 Drugs. *N Engl J Med* **2022**, *387*, 654-655.

46. Shafiee, A.; Teymouri Athar, M.M.; Kohandel Gargari, O.; Jafarabady, K.; Siahvoshi, S.; Mozhgani, S.-H. Ivermectin under scrutiny: a systematic review and meta-analysis of efficacy and possible sources of controversies in COVID-19 patients. *Virology Journal* **2022**, *19*, 102.

47. Au Sam, H.; Storey Brian, D.; Moore John, C.; Tang, Q.; Chen, Y.-L.; Javaid, S.; Sarioglu, A.F.; Sullivan, R.; Madden Marissa, W.; O'Keefe, R.; et al. Clusters of circulating tumor cells traverse capillary-sized vessels. *Proceedings of the National Academy of Sciences* **2016**, *113*, 4947-4952.

48. Yamakawa, N.; Vanbeselaere, J.; Chang, L.-Y.; Yu, S.-Y.; Ducrocq, L.; Harduin-Lepers, A.; Kurata, J.; Aoki-Kinoshita, K.F.; Sato, C.; Khoo, K.-H.; et al. Systems glycomics of adult zebrafish identifies organ-specific sialylation and glycosylation patterns. *Nature Communications* **2018**, *9*, 4647.

49. Zheng, Y.; Zhao, J.; Li, J.; Guo, Z.; Sheng, J.; Ye, X.; Jin, G.; Wang, C.; Chai, W.; Yan, J.; et al. SARS-CoV-2 spike protein causes blood coagulation and thrombosis by competitive binding to heparan sulfate. *Int J Biol Macromol* **2021**, *193*, 1124-1129.

50. Colunga Biancatelli, R.M.L.; Solopov, P.A.; Sharlow, E.R.; Lazo, J.S.; Marik, P.E.; Catravas, J.D. The SARS-CoV-2 spike protein subunit S1 induces COVID-19-like acute lung injury in K18-hACE2 transgenic mice and barrier dysfunction in human endothelial cells. *Am J Physiol Lung Cell Mol Physiol* **2021**, *321*, L477-l484.

51. Nuovo, G.J.; Magro, C.; Shaffer, T.; Awad, H.; Suster, D.; Mikhail, S.; He, B.; Michaille, J.-J.; Liechty, B.; Tili, E. Endothelial cell damage is the central part of COVID-19 and a mouse model induced by injection of the S1 subunit of the spike protein. *Annals of Diagnostic Pathology* **2021**, *51*, 151682.

52. Perico, L.; Morigi, M.; Galbusera, M.; Pezzotta, A.; Gastoldi, S.; Imberti, B.; Perna, A.; Ruggenenti, P.; Donadelli, R.; Benigni, A.; et al. SARS-CoV-2 Spike Protein 1 Activates Microvascular Endothelial Cells and Complement System Leading to Platelet Aggregation. *Front Immunol* **2022**, *13*, 827146.

53. Fantini, J.; Yahi, N.; Colson, P.; Chahinian, H.; La Scola, B.; Raoult, D. The puzzling mutational landscape of the SARS-2-variant Omicron. *Journal of Medical Virology* **2022**, *94*, 2019-2025.

54. Price, L.C.; McCabe, C.; Garfield, B.; Wort, S.J. Thrombosis and COVID-19 pneumonia: the clot thickens! *European Respiratory Journal* **2020**, *56*, 2001608.

55. Maslo, C.; Friedland, R.; Toubkin, M.; Laubscher, A.; Akaloo, T.; Kama, B. Characteristics and Outcomes of Hospitalized Patients in South Africa During the COVID-19 Omicron Wave Compared With Previous Waves. *JAMA* **2022**, *327*, 583-584.

56. Lang, Y.; Li, W.; Li, Z.; Koerhuis, D.; van den Burg, A.C.S.; Rozemuller, E.; Bosch, B.-J.; van Kuppeveld, F.J.M.; Boons, G.-J.; Huizinga, E.G.; et al. Coronavirus hemagglutinin-esterase and spike proteins coevolve for functional balance and optimal virion avidity. *Proc Natl Acad Sci USA* **2020**, *117*, 25759-25770.

57. Kumar, S.; Karuppanan, K.; Subramaniam, G. Omicron (BA.1) and sub-variants (BA.1.1, BA.2, and BA.3) of SARS-CoV-2 spike infectivity and pathogenicity: A comparative sequence and structural-based computational assessment. *Journal of Medical Virology* **2022**, *94*, 4780-4791.

58. Pascarella, S.; Ciccozzi, M.; Bianchi, M.; Benvenuto, D.; Cauda, R.; Cassone, A. The value of electrostatic potentials of the spike receptor binding and N-terminal domains in addressing transmissibility and infectivity of SARS-CoV-2 variants of concern. *J Infect* **2022**, *84*, e62-e63.

59. Lam, S.D.; Waman, V.P.; Orengo, C.; Lees, J. Insertions in the SARS-CoV-2 Spike N-Terminal Domain May Aid COVID-19 Transmission. *bioRxiv* **2021**, doi:10.1101/2021.12.06.471394.

60. Doria, D.; Santin, A.D.; Tuszynski, J.A.; Scheim, D.E.; Aminpour, M. Omicron SARS-CoV-2 Spike-1 Protein's Decreased Binding Affinity to α7nAChr: Implications for Autonomic Dysregulation of the Parasympathetic Nervous System and the Cholinergic Anti-Inflammatory Pathway—An In Silico Analysis. *BioMedInformatics* **2022**, *2*, 553-564.

61. M. Yagisawa and S. Omura, personal communication (email) of November 7, 2022.

62. Stone, J.C.; Ndarukwa, P.; Scheim, D.E.; Dancis, B.M.; Dancis, J.; Gill, M.G.; Aldous, C. Changes in SpO2 on Room Air for 34 Severe COVID-19 Patients after Ivermectin-Based Combination Treatment: 62% Normalization within 24 Hours. *Biologics* **2022**, *2*, 196-210.

63. Gupta, Y.; Maciorowski, D.; Zak, S.E.; Kulkarni, C.V.; Herbert, A.S.; Durvasula, R.; Fareed, J.; Dye, J.M.; Kempaiah, P. Heparin: A simplistic repurposing to prevent SARS-CoV-2 transmission in light of its in-vitro nanomolar efficacy. *Int J Biol Macromol* **2021**, *183*, 203-212.

64. Li, C.; Chen, Y.; Zhao, Y.; Lung, D.C.; Ye, Z.; Song, W.; Liu, F.-F.; Cai, J.-P.; Wong, W.-M.; Yip, C.C.-Y.; et al. Intravenous Injection of Coronavirus Disease 2019 (COVID-19) mRNA Vaccine Can Induce Acute Myopericarditis in Mouse Model. *Clinical Infectious Diseases* **2022**, *74*, 1933-1950.

65. Trougakos, I.P.; Terpos, E.; Alexopoulos, H.; Politou, M.; Paraskevis, D.; Scorilas, A.; Kastritis, E.; Andreakos, E.; Dimopoulos, M.A. Adverse effects of COVID-19 mRNA vaccines: the spike hypothesis. *Trends in Molecular Medicine* **2022**, *28*, 542-554.

66. Cosentino, M.; Marino, F. The spike hypothesis in vaccine-induced adverse effects: questions and answers. *Trends in Molecular Medicine* **2022**, *28*, 797-799.

67. Cognetti, J.S.; Miller, B.L. Monitoring Serum Spike Protein with Disposable Photonic Biosensors Following SARS-CoV-2 Vaccination. *Sensors* **2021**, *21*, 5857.

68. Ogata, A.F.; Cheng, C.A.; Desjardins, M.; Senussi, Y.; Sherman, A.C.; Powell, M.; Novack, L.; Von, S.; Li, X.; Baden, L.R.; et al. Circulating Severe Acute Respiratory Syndrome Coronavirus 2 (SARS-CoV-2) Vaccine Antigen Detected in the Plasma of mRNA-1273 Vaccine Recipients. *Clin Infect Dis* **2022**, *74*, 715-718.

69. Röltgen, K.; Nielsen, S.C.A.; Silva, O.; Younes, S.F.; Zaslavsky, M.; Costales, C.; Yang, F.; Wirz, O.F.; Solis, D.; Hoh, R.A.; et al. Immune imprinting, breadth of variant recognition, and germinal center response in human SARS-CoV-2 infection and vaccination. *Cell* **2022**, *185*, 1025-2040.

70. Giovannini, F. Dark Field Microscopic Analysis on the Blood of 1,006 Symptomatic Persons After Anti-COVID mRNA Injections from Pfizer/BioNTech or Moderna. *International Journal of Vaccine Theory, Practice, and Research* **2022**, *2*, 385-444.

71. Mansanguan, S.; Charunwatthana, P.; Piyaphanee, W.; Dechkhajorn, W.; Poolcharoen, A.; Mansanguan, C. Cardiovascular Manifestation of the BNT162b2 mRNA COVID-19 Vaccine in Adolescents. *Tropical Medicine and Infectious Disease* **2022**, *7*, 196.

72. Klotz, U.; Ogbuokiri, J.E.; Okonkwo, P.O. Ivermectin binds avidly to plasma proteins. *Eur J Clin Pharmacol* **1990**, *39*, 607-608.

73. Colson, P.; Levasseur, A.; Delerce, J.; Pinault, L.; Dudouet, P.; Devaux, C.; Fournier, P.E.; La Scola, B.; Lagier, J.C.; Raoult, D. Spreading of a new SARS-CoV-2 N501Y spike variant in a new lineage. *Clin Microbiol Infect* **2021**, *27*, 1352.e1351-1352.e1355.

74. Jaafar, R.; Boschi, C.; Aherfi, S.; Bancod, A.; Le Bideau, M.; Edouard, S.; Colson, P.; Chahinian, H.; Raoult, D.; Yahi, N.; et al. High Individual Heterogeneity of Neutralizing Activities against the Original Strain and Nine Different Variants of SARS-CoV-2. *Viruses* **2021**, *13*, doi:10.3390/v13112177.

75. Boschi, C.; Colson, P.; Bancod, A.; Moal, V.; La Scola, B. Omicron Variant Escapes Therapeutic Monoclonal Antibodies (mAbs) Including Recently Released Evusheld®, Contrary to 8 Prior Main Variant of Concern (VOC). *Clinical Infectious Diseases* **2022**, *75*, e534-e535.

76. Rambaut, A.; Holmes, E.C.; O'Toole, Á.; Hill, V.; McCrone, J.T.; Ruis, C.; du Plessis, L.; Pybus, O.G. A dynamic nomenclature proposal for SARS-CoV-2 lineages to assist genomic epidemiology. *Nature Microbiology* **2020**, *5*, 1403-1407.

77. Townsend, A.; Rijal, P.; Xiao, J.; Tan, T.K.; Huang, K.A.; Schimanski, L.; Huo, J.; Gupta, N.; Rahikainen, R.; Matthews, P.C.; et al. A haemagglutination test for rapid detection of antibodies to SARS-CoV-2. *Nat Commun* **2021**, *12*, 1951.

78. Fantini, J.; Yahi, N.; Azzaz, F.; Chahinian, H. Structural dynamics of SARS-CoV-2 variants: A health monitoring strategy for anticipating Covid-19 outbreaks. *J Infect* **2021**, *83*, 197-206.

79. Kim, D.E.; Chivian, D.; Baker, D. Protein structure prediction and analysis using the Robetta server. *Nucleic Acids Res* **2004**, *32*, W526-531.

80. Guex, N.; Peitsch, M.C. SWISS-MODEL and the Swiss-PdbViewer: an environment for comparative protein modeling. *Electrophoresis* **1997**, *18*, 2714-2723.